

## Direct Measurement of the Lifetime of Optical Phonons in Single-Walled Carbon Nanotubes

Daohua Song,<sup>1</sup> Feng Wang,<sup>1,\*</sup> Gordana Dukovic,<sup>2</sup> M. Zheng,<sup>3</sup> E. D. Semke,<sup>3</sup> Louis E. Brus,<sup>2</sup> and Tony F. Heinz<sup>1,†</sup>

<sup>1</sup>*Departments of Physics and Electrical Engineering, Columbia University, New York, New York 10027, USA*

<sup>2</sup>*Department of Chemistry, Columbia University, New York, New York 10027, USA*

<sup>3</sup>*DuPont Central Research and Development, Wilmington, Delaware 19880, USA*

(Received 1 August 2007; revised manuscript received 31 October 2007; published 4 June 2008)

Time-resolved anti-Stokes Raman spectroscopy has been applied to probe the dynamics of optical phonons created in single-walled carbon nanotubes by femtosecond laser excitation. From measurement of the decay of the anti-Stokes Raman signal in semiconducting nanotubes of (6, 5) chiral index, a room-temperature lifetime for *G*-mode phonons of  $1.1 \pm 0.2$  ps has been determined. This lifetime, which reflects the anharmonic coupling of the *G*-mode phonons to lower-frequency phonons, is important in assessing the role of nonequilibrium phonon populations in high-field transport phenomena.

DOI: 10.1103/PhysRevLett.100.225503

PACS numbers: 63.20.K-, 78.30.-j, 78.47.jc, 78.67.Ch

Single-walled carbon nanotubes (SWNTs) provide an ideal system in which to explore the physical properties of highly one-dimensional materials and the interaction of their fundamental excitations [1]. In this context, electron-electron interactions have been studied in several distinct contexts, including Luttinger-liquid behavior and exciton formation [2–4]. There has also been intensive investigation of electron-phonon interactions, which allow Raman scattering and are of critical importance for charge transport processes. Strong electron-phonon coupling is known to occur for optical phonons, especially for phonons near the  $\Gamma$  and *K* points in the Brillouin zone [5–7]. On the other hand, there is little direct experimental information about *phonon-phonon interactions* in carbon nanotubes. In addition to the critical role of phonon-phonon interactions in thermal transport, these interactions have recently attracted attention because of the possibility of nonequilibrium phonon populations being developed in SWNTs under high-current transport conditions [8–13]. In particular, nonequilibrium optical phonon populations have been invoked to explain the current saturation and negative differential resistance observed in electrical transport experiments [10,11,13]. The role of nonequilibrium phonons depends sensitively on the lifetime of phonons against anharmonic decay into lower-energy phonons. This lifetime determines the degree to which nonequilibrium populations are created and sustained.

In this Letter, we present a direct determination of the population lifetime of optical phonons in semiconducting carbon nanotubes. The experimental approach is based on time-resolved anti-Stokes Raman (ASR) scattering [14]. Anti-Stokes Raman scattering provides a sensitive probe of high-energy phonons since the ASR signal scales directly with the phonon population. Here we apply ASR as a time-domain probe of the nonequilibrium population of optical phonons created in carbon nanotubes by a femtosecond pump pulse. For semiconducting nanotubes of (6, 5) chiral index, the room-temperature lifetime for *G*-mode phonons [1], the optical phonons near the  $\Gamma$  point of the Brillouin zone, is found to be  $1.1 \pm 0.2$  ps. This result is compatible

with previously determined values of the Raman linewidth [15]. These latter measurements, however, provide only a lower bound on the lifetime of *G*-mode phonons since the linewidth can include contributions from inhomogeneous broadening and pure dephasing in addition to lifetime broadening.

Our sample of SWNTs was prepared by chemical vapor deposition using the CoMo alloy catalyst (CoMoCAT) process [16]. This step was followed by DNA-assisted dispersion and separation [17] to yield isolated SWNTs, predominantly of (6, 5) chiral structure. Figure 1 shows the measured optical absorption spectrum  $\alpha_0(\hbar\omega)$  of the SWNTs suspended in D<sub>2</sub>O for photon energies  $\hbar\omega$  between 1.1 and 2.3 eV. The principal feature at 1.25 eV arises from the *E*<sub>11</sub> exciton in the (6, 5) nanotubes. The weak peak from 1.4 to 1.5 eV arises from the corresponding

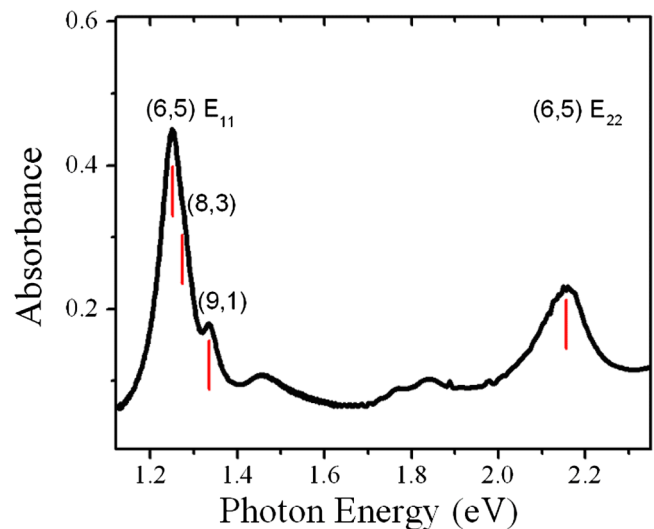


FIG. 1 (color online). Absorption spectrum of the SWNT suspension in a 1-cm cell of D<sub>2</sub>O. The positions of the *E*<sub>11</sub> (1.25 eV) and *E*<sub>22</sub> (2.16 eV) transitions of the (6, 5) nanotubes are indicated, as are the *E*<sub>11</sub> transitions in the minority (8, 3) and (9, 1) nanotubes. The peak between 1.4–1.5 eV is the phonon sideband of the *E*<sub>11</sub> transition in the (6, 5) nanotubes.

phonon-assisted transition [7]. The other weak features from 1.3–1.38 eV are  $E_{11}$  transitions in minority nanotube species, assigned to (8, 3) and (9, 1) structures [18].

The apparatus for the pump-probe measurements was based on a 1-kHz regeneratively amplified, modelocked Ti:sapphire laser and an optical parametric generator that produced tunable laser pulses of  $\sim 100$ -fs duration. Probe radiation at a photon energy of 2.17 eV was chosen to benefit from resonant enhancement of the Raman signal through the  $E_{22}$  transition in the (6, 5) nanotubes. For pump radiation we directly used the amplified Ti:sapphire laser pulses, which, at a photon energy of 1.55 eV, were in resonance with the phonon-assisted  $E_{11}$  transition in the (6, 5) nanotubes [7]. We verified that we were indeed exciting the (6, 5) nanotubes by observing that the fluorescence was dominated by the  $E_{11}$  emission feature of the (6, 5) nanotubes. All measurements were performed at room temperature with pump and probe radiation of parallel linear polarization.

For the near-armchair (6, 5) nanotubes used in our study, the Raman spectrum is dominated by the  $G^+$  mode, corresponding to zone-center longitudinal optical phonons [19]. Figure 2(a) displays the Stokes Raman spectrum measured with our femtosecond probe pulses. The large observed width reflects the spectral bandwidth of the probe pulses, as constrained by their femtosecond duration, rather than the intrinsic nanotube Raman response. Figure 2(b) shows the corresponding anti-Stokes portion of the Raman spectrum, both with and without the application of simultaneous pump radiation. For ASR scattering, the measured signal scales directly with the phonon mode population  $n$ . In the absence of pump radiation, only a weak ASR signal is observed [lower curve in Fig. 2(b)]. Application of coincident pump radiation yields, however, a much stronger anti-Stokes Raman signal [upper curve in Fig. 2(b)].

Adjusting for the efficiency of the detection system at different wavelengths, we obtain an anti-Stokes to Stokes intensity ratio of  $I_{AS}/I_S = 0.045$  for probe pulses coincident in time with pump pulses of  $1.0 \text{ J m}^{-2}$  fluence. From this ratio, we may infer the phonon mode population  $n$  and the corresponding effective temperature. For the optically thin sample relevant in our measurements, we can determine the phonon population from the relation  $I_{AS}/I_S = (\omega_{AS}/\omega_S)^4 [n/(n+1)] [(\omega_S - \omega_0 + i\Gamma_0/2)/(\omega_{AS} - \omega_0 + i\Gamma_0/2)]^2$ . Here  $\omega_S$ ,  $\omega_{AS}$  denote the Stokes and anti-Stokes emission frequencies;  $\omega_0$  and  $\Gamma_0$  describe, respectively, the center frequency and FWHM of the  $E_{22}$  transition excited by the probe laser, and the indicated functional form for the Raman response has been previously used to describe Raman excitation profiles in nanotubes [20]. From this analysis, we deduce a maximum effective temperature of 680 K for the  $G$  mode immediately after excitation by a pump pulse. (In the absence of the pump radiation, the probe pulse itself induces a moderate increase in the  $G$ -mode effective temperature, but only by 160 K.) If we assume that the femtosecond pump pulses produce equilibrium heating of the nanotubes, we obtain, on the other hand, a temperature rise of  $< 10$  K. This estimate is derived using the absorbed energy (from the pump fluence and the nanotube absorption cross section [21]) and the nanotube specific heat [22]. The much higher effective temperature for the  $G$ -mode phonons demonstrates directly that the pump pulses create a significant *nonequilibrium* population in this mode.

The dynamical properties of these nonequilibrium  $G$ -mode phonons are examined by recording the ASR signal as a function of the delay  $\Delta t$  of the probe pulse with respect to the pump pulse. As shown in Fig. 3, we observe a sharp rise in the ASR signal, followed by decay on the time scale of 1 ps. We can analyze the response using a simple model in which the phonon population rises

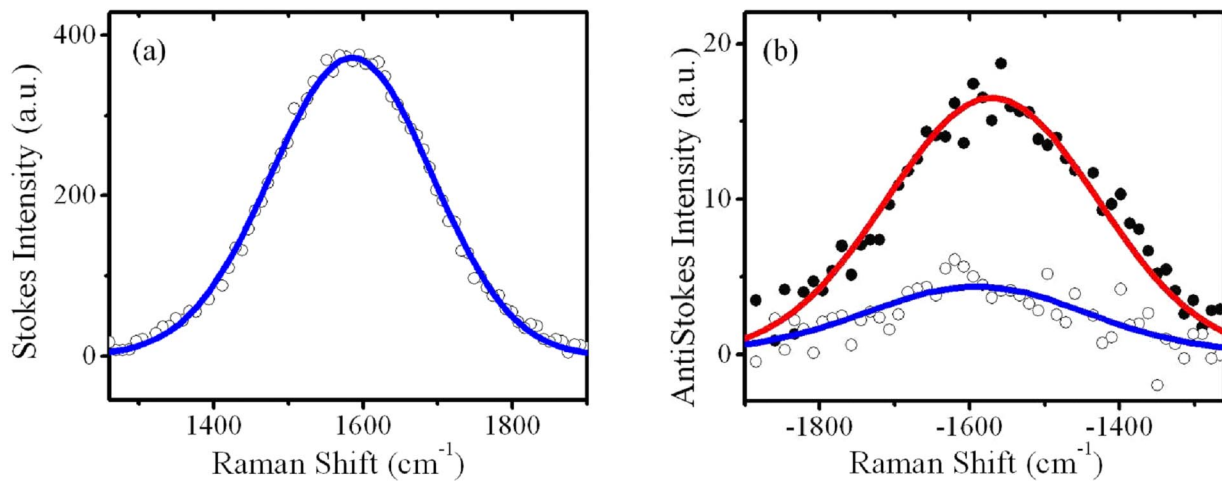


FIG. 2 (color online). Stokes and anti-Stokes Raman spectra of  $G$ -mode phonons measured with femtosecond probe pulses at 2.17 eV. The solid lines are fits to Gaussian functions with a width reflecting that of the probe pulses. (a) Spectrum for Stokes Raman scattering. The signal is independent of the presence or absence of a time-synchronized femtosecond pump beam. (b) Spectrum for anti-Stokes Raman scattering in the presence (filled circles) and absence (open circles) of pump pulses.

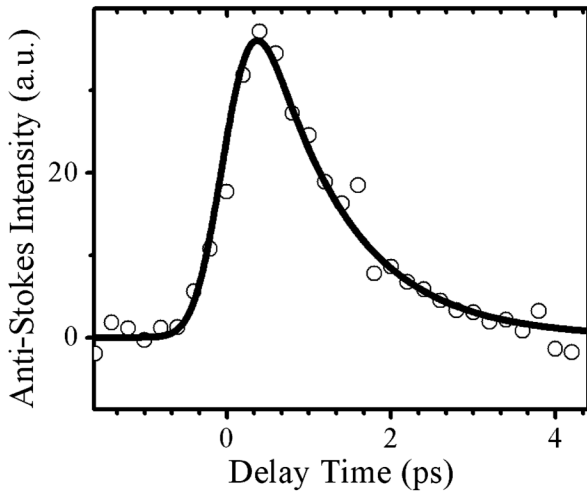


FIG. 3. Time evolution of  $G$ -mode anti-Stokes Raman signal (symbols) as a function of probe delay after the pump pulse. The solid curve is obtained from a model that assumes instantaneous generation of hot phonons, but takes into account the finite instrumental time resolution (defining the rise time) and phonon lifetime (defining the decay time). A  $G$ -mode phonon lifetime of  $\tau = 1.1 \pm 0.2$  ps is deduced.

instantaneously with the integrated pump intensity and then decays exponentially. Taking into account the finite duration of the probe pulse, we obtain a good fit to the data (solid curve in Fig. 3) and infer a time constant of  $\tau = 1.1 \pm 0.2$  ps for the population lifetime of the  $G$ -mode phonons. This decay time was found to be independent of the pump excitation density for the measured range of fluences between 0.5 and 1.5 J m<sup>-2</sup>.

Before considering the  $G$ -mode lifetime, we briefly discuss the rapid buildup of the nonequilibrium population. The  $G$ -mode phonons are produced by two mechanisms. In the first process, we instantaneously generate an optical phonon upon absorption of a photon, since we excite the phonon sideband of the  $E_{11}$  exciton [5,7]. A second mechanism for optical phonon generation is through the exciton-exciton annihilation process in which a pair of  $E_{11}$  excitons merges to produce a single high-energy electron-hole pair [23]. This excitation cools by the emission of phonons, with strong coupling expected for optical phonons near the  $\Gamma$  and the  $K$  points [5–7]. Although the phonon emission time is not directly known, the optically produced excitons in higher subbands relax to the  $E_{11}$  subband in less than 100 fs [24]. The sharp rise of the ASR signal implies that the exciton-exciton annihilation process is also very fast. For our typical pump fluence of 1.0 J m<sup>-2</sup>, we produce  $\sim 10$  excitons per micron in each nanotube [21], suggesting exciton-exciton annihilation on a subpicosecond time scale [25].

We now discuss the decay channels leading to the measured  $G$ -mode phonon lifetime. We first note that the lifetime broadening for the  $G$ -mode phonons implied by the measured population lifetime of  $\tau = 1.1 \pm 0.2$  ps is  $\Gamma = 4.8$  cm<sup>-1</sup> (FWHM). This value is consistent with conven-

tional Raman scattering data in which the  $G^+$  linewidth of semiconducting nanotubes is found to exceed 6 cm<sup>-1</sup> [15], even for isolated, freely suspended nanotubes. The larger observed linewidth in these frequency-domain measurements reflects contributions of pure dephasing processes and inhomogeneous broadening.

How is the energy of the  $G$ -mode optical phonons dissipated in the measured 1.1 ps? In metallic SWNTs, electronic excitations provide a significant (nonadiabatic) channel for relaxation of  $G$ -mode phonons [13,26]. For the (6, 5) semiconducting nanotubes, however, the minimum energy for interband transitions exceeds 1 eV, so the optical phonons with 0.2 eV energy will not couple efficiently to these excitations. It is also appropriate to ask whether the phonons may relax through coupling to *photo-generated* electronic excitations. For the conditions of our experiment, this possibility can also be ruled out: The observed phonon decay rate is independent of the pump fluence and hence of the density of photogenerated electronic excitations. This latter result is not unexpected, since the typical density of photogenerated carriers for our experiment is only  $\sim (100 \text{ nm})^{-1}$ , far below the density of carriers in metallic nanotubes. We deduce that the observed decay of the  $G$ -mode phonons must occur through the generation of lower-energy phonons, i.e., through anharmonic mode coupling.

The nanotube  $G$ -mode phonons could in principle decay directly into vibrational excitations of the molecules surrounding the nanotube. Experiments have demonstrated that the thermal energy flow from phonons in SWNTs to the surrounding surfactant and solvent (water) molecules occurs in tens of picoseconds [27]. According to molecular dynamics simulations on short segments of nanotubes [28], higher-energy phonons have even weaker coupling to the surroundings than the low-frequency thermal phonons. To support this conclusion experimentally, we performed time-resolved Raman measurements of the  $G$ -mode lifetime on nanotubes suspended in D<sub>2</sub>O using two different surfactants, sodium dodecylbenzene sulfonate and sodium cholate. No meaningful difference in the phonon dynamics was observed. We conclude that the intranantube processes dominate decay of the  $G$ -mode phonons.

Possible processes for the anharmonic decay of the  $G$ -mode phonons can be identified by examination of the calculated phonon dispersion relations [29]. Several decay channels producing two phonons can be identified that would conserve both energy and momentum. These include production of two acoustic phonons of opposite momentum and, because of the strong dispersion of the optical phonons, the generation of an optical phonon away from the zone center and of an acoustic phonon of opposite momentum.

An interesting point of comparison for the present result is with the behavior of phonons in graphite. The room-temperature lifetime of  $G$ -mode phonons in graphite has been recently predicated theoretically to be  $\sim 3$  ps [30]. From terahertz spectroscopy probing the relaxation of the

electronic temperature in graphite following pulsed excitation, an effective lifetime of the combined  $G$ - and  $K$ -point phonons was estimated to be several picoseconds [31]. While these experimental data do not provide a direct comparison, the results suggest that the lifetime of  $G$ -mode phonons in graphite exceeds that in nanotubes. In addition to the altered densities of states and selection rules, a possible explanation for an increased decay rate for nanotubes is the existence of additional, distinctive phonon modes. In particular, recent experiments have demonstrated a strong coupling of  $G$ -mode phonons to radial breathing mode phonons [32], a process that opens up a decay channel in nanotubes that is absent in graphite.

Because of the strong interaction of the zone-center optical phonons with charge carriers in nanotubes, the population of these phonons is expected to play an important role in electrical transport. The lifetime for optical phonons of 1.1 ps found in this investigation should help to elucidate the role of nonequilibrium phonon populations. Under conditions of current flow, a dynamic equilibrium is reached between electrons and optical phonons through the electron-phonon interaction, with the anharmonic phonon decay rate controlling the degree of buildup of a nonthermal phonon population. An increase of the high-current differential resistance by a factor of 3 has, for example, been predicted for an optical phonon lifetime of 5 ps compared to the behavior for a 1-ps lifetime [13]. This difference arises from the increased optical phonon population and accompanying enhanced electron scattering for the longer phonon lifetime. The anharmonic phonon decay rate is also expected to play an important role in the recently reported electroluminescence in semiconducting SWNTs induced by unipolar charge transport [33,34]. In this instance, light emission is attributed to impact exciton generation by hot carriers. This process is a strong function of the energy distribution of the charge carriers, which in turn depends sensitively on the optical phonon population [35].

In conclusion, we have applied time-resolved anti-Stokes Raman scattering to determine directly the population lifetime of  $G$ -mode optical phonons in (6,5) semiconducting single-walled carbon nanotubes. The lifetime for anharmonic decay of these zone-center optical phonons is found to be  $1.1 \pm 0.2$  ps. In addition to its relevance in understanding phonon-phonon interactions in nanotubes, this result has implications for the role of nonequilibrium phonon populations in high-current electrical transport.

We thank Dr. Yi Rao for experimental support and acknowledge support from the Nanoscale Science and Engineering Initiative of the NSF under Grants No. CHE-0117752 and No. ECS-05-07111, the New York State Office of Science, Technology, and Academic Research (NYSTAR), and the Office of Basic Energy Sciences, U.S. DOE under Grants No. DE-FG02-98ER-14861 and No. DE-FG02-03ER15463.

\*Current address: Department of Physics, University of California, Berkeley, CA 94720, USA.

†Corresponding author.  
tony.heinz@columbia.edu

- [1] R. Saito, G. Dresselhaus, and M. S. Dresselhaus, *Physical Properties of Carbon Nanotubes* (Imperial College Press, London, 1998); S. Reich, C. Thomsen, and J. Maultzsch, *Carbon Nanotubes: Basic Concepts and Physical Properties* (Wiley, New York, 2004).
- [2] M. Bockrath *et al.*, Nature (London) **397**, 598 (1999).
- [3] F. Wang *et al.*, Science **308**, 838 (2005).
- [4] J. Maultzsch *et al.*, Phys. Rev. B **72**, 241402 (2005).
- [5] V. Perebeinos, J. Tersoff, and P. Avouris, Phys. Rev. Lett. **94**, 027402 (2005).
- [6] J. Y. Park *et al.*, Nano Lett. **4**, 517 (2004).
- [7] S. G. Chou *et al.*, Phys. Rev. Lett. **94**, 127402 (2005); H. Htoon *et al.*, Phys. Rev. Lett. **94**, 127403 (2005); F. Plentz *et al.*, Phys. Rev. Lett. **95**, 247401 (2005).
- [8] Z. Yao, C. L. Kane, and C. Dekker, Phys. Rev. Lett. **84**, 2941 (2000).
- [9] V. Perebeinos, J. Tersoff, and P. Avouris, Phys. Rev. Lett. **94**, 086802 (2005).
- [10] E. Pop *et al.*, Phys. Rev. Lett. **95**, 155505 (2005).
- [11] M. Lazzeri *et al.*, Phys. Rev. Lett. **95**, 236802 (2005).
- [12] A. Javey *et al.*, Phys. Rev. Lett. **92**, 106804 (2004).
- [13] M. Lazzeri and F. Mauri, Phys. Rev. B **73**, 165419 (2006).
- [14] J. A. Kash, J. C. Tsang, and J. M. Hvam, Phys. Rev. Lett. **54**, 2151 (1985); K. T. Tsen *et al.*, Phys. Rev. B **39**, 1446 (1989).
- [15] A. Jorio *et al.*, Phys. Rev. B **66**, 115411 (2002); M. S. Dresselhaus *et al.*, Carbon **40**, 2043 (2002); J. C. Meyer *et al.*, Phys. Rev. Lett. **95**, 217401 (2005).
- [16] S. M. Bachilo *et al.*, J. Am. Chem. Soc. **125**, 11186 (2003).
- [17] M. Zheng *et al.*, Science **302**, 1545 (2003).
- [18] M. S. Arnold, S. I. Stupp, and M. C. Hersam, Nano Lett. **5**, 713 (2005).
- [19] S. G. Chou *et al.*, Chem. Phys. Lett. **397**, 296 (2004).
- [20] A. Compaan and H. J. Trodahl, Phys. Rev. B **29**, 793 (1984).
- [21] M. F. Islam *et al.*, Phys. Rev. Lett. **93**, 037404 (2004).
- [22] J. Hone *et al.*, Science **289**, 1730 (2000).
- [23] F. Wang *et al.*, Phys. Rev. B **70**, 241403 (2004).
- [24] C. Manzoni *et al.*, Phys. Rev. Lett. **94**, 207401 (2005).
- [25] F. Wang *et al.*, Phys. Rev. B **73**, 245424 (2006).
- [26] Y. Wu *et al.*, Phys. Rev. Lett. **99**, 027402 (2007).
- [27] S. T. Huxtable *et al.*, Nat. Mater. **2**, 731 (2003).
- [28] S. Shenogin *et al.*, J. Appl. Phys. **95**, 8136 (2004).
- [29] J. Maultzsch *et al.*, Solid State Commun. **121**, 471 (2002); E. Dobardzic *et al.*, Phys. Rev. B **68**, 045408 (2003).
- [30] N. Bonini *et al.*, Phys. Rev. Lett. **99**, 176802 (2007).
- [31] T. Kampfrath *et al.*, Phys. Rev. Lett. **95**, 187403 (2005).
- [32] A. Gambetta *et al.*, Nature Phys. **2**, 515 (2006).
- [33] L. Marty *et al.*, Phys. Rev. Lett. **96**, 136803 (2006).
- [34] J. Chen *et al.*, Science **310**, 1171 (2005).
- [35] V. Perebeinos and P. Avouris, Phys. Rev. B **74**, 121410 (2006).